PHYSICAL REVIEW D
PARTICLES AND FIELDS

THIRD SERIES, VOLUME 34, NUMBER 10 15 NOVEMBER 1986

Inflation and bubbles in general relativity

Pablo Laguna-Castillo and Richard A. Matzner
Center for Relativity and Physics Department, The University of Texas at Austin, Austin, Texas 78712
(Received 5 May 1986)

Following Israel's study of singular hypersurfaces and thin shells in general relativity, the complete set of Einstein's field equations in the presence of a bubble boundary Σ is reviewed for all spherically symmetric embedding four-geometries $M^{\pm}$. The mapping that identifies points between the boundaries Σ^+ and Σ^- is obtained explicitly when the regions M^+ and M^- are described by a de Sitter and a Minkowski metric, respectively. In addition, the evolution of a bubble with vanishing surface energy density is studied in a spatially flat Robertson-Walker space-time, for region M^- radiation dominated with a vanishing cosmological constant, and an energy equation in M^+ determined by the matching. It is found that this type of bubble leads to a "worm-hole" matching; that is, an infinite extent exterior of a sphere is joined across the wall to another infinite extent exterior of a sphere. Interior-interior matches are also possible. Under this model, solutions for a bubble following a Hubble law are analyzed. Numerical solutions for bubbles with constant tension are also obtained.

I. INTRODUCTION

In the last few years, vacuum phase transitions have been a subject of great interest because of their notable implications for cosmology.[1] The transitions are triggered by the nucleation of true vacuum bubbles that expand converting a false vacuum into a true vacuum as they grow.

The problem of the growth of these bubbles, with a complete consideration of gravitational effects, seems to be extremely complicated. The analysis of Coleman and De Luccia[2] on vacuum decay shows that gravitational effects are not negligible in the bubble's growth. Recently, Lake[3] and Berezin, Kuzmin, and Tkachev[4] have discussed the evolution of a single bubble, where the bubble is idealized as a thin spherically symmetric shell. Collisions of two bubbles have been investigated by Hawking, Moss, and Stewart[5] in a flat space-time, and by Chao[6] with the inclusion of gravitational effects. However, despite its importance, the problem of the junction conditions on phase separation boundaries has been hardly discussed.[7] In particular, there has been no study of the mapping that identifies points in the bubble's wall (in general, the space-time is described by different metrics inside and outside the shell).

In this paper we shall study a single bubble as a phase separation wall. In order to apply Israel's formalism of singular hypersurfaces and thin shells,[8] we will assume that the "thin wall" approximation holds through the evolution of the bubble. (This assumption is not valid for bubbles in the new inflationary scenario.[9]) We begin in Sec. II with a review of surfaces of discontinuity. Special care is given to the continuity and discontinuity behavior of tensorial quantities since, in general, the two disjoint submanifolds M^+ and M^-, into which the space-time is divided by the hypersurface, have mutually independent coordinate charts. We also recall the complete set of equations to solve Einstein's equations in the presence of a hypersurface of discontinuity. Our study of a bubble will be based on this set of equations with two main purposes: to investigate the history of the wall and to obtain the mapping that effects the join across the hypersurface.

In Sec. III the formalism for surfaces of discontinuity is applied to spherically symmetric shells. The equations that completely determine the history of the bubble wall are obtained in a form similar to those of Lake.[3] As a first example, we investigate a vacuum bubble; that is, a bubble that materializes in the decay of a false vacuum. In particular, we obtain the explicit form of the mapping that identifies points in the wall of the shell. It is found that this mapping can be extended beyond the event horizon of the de Sitter space-time in which the bubble is immersed.

In Sec. IV we consider the case of a nonvacuum bubble when the space-time is given by a spatially flat Friedmann-Robertson-Walker (FRW) metric. We suppose that the bubble has a vanishing surface energy density, which leads to the conservation of energy and momentum flux across the wall (detonation wave approximation). In addition, there is a nonvanishing vacuum energy in

M^+, and the medium in M^- is radiation dominated with a vanishing vacuum energy. It is found that the spatially flat FRW space-time and vanishing surface energy density assumptions lead to a bubble with "worm-hole" characteristics. That is, the bubble joins either exterior or interior regions of spheres with radius equal to that of the bubble. We discuss the evolution of such a bubble in the case that its expansion follows a Hubble law. In this case, the demand of finite-wall tension coincides with the imposition of the weak-energy condition in M^+ and requires the radius of the bubble to be finite and larger than the event horizon in M^- throughout its expansion. In addition, the region M^+ experiences an inflation era as we approach the maximum radius of the bubble. Finally, we obtain numerical solutions for bubbles with constant tension. We find that depending on the worm-hole matching, on the negative or positive tension, and on the other initial data, the bubble after nucleation could expand forever, shrink, or grow up to a maximum radius and then contract.

II. SURFACES OF DISCONTINUITY

Following Israel's study of singular hypersurfaces and thin shells in general relativity,[8] we shall use the Gauss-Codazzi formalism to obtain Einstein's equations in the presence of stress-energy sources confined to three-dimensional timelike hypersurfaces (surface layers). Special attention is paid to the continuity and discontinuity behavior of the quantities across the hypersurface since, besides the dynamics of the hypersurface, we will be interested in the match of the two submanifolds into which the space-time is divided. We will review the set of general equations that solve Einstein's equations for an arbitrary hypersurface, and later we will apply this set to the spherically symmetric case.

A. Metric continuity

Let Σ denote a three-dimensional timelike hypersurface, which divides space-time into two disjoint four-dimensional submanifolds M^+,M^- with boundaries Σ^+, Σ^- and metrics g^+_{ab}, g^-_{ab}, respectively (latin indices take the range 0,1,2,3). In order to have a unique intrinsic geometry at Σ, both g^+_{ab} and g^-_{ab} must induce the same intrinsic metric on Σ; in other words, the metric must be continuous across the imbedded hypersurface, which means that distances measured on Σ^+ and Σ^- must agree.

It is very important to point out that great care should be taken whenever one speaks about continuities or discontinuities of tensorial quantities because, in general, mutually independent coordinate charts, x^+_a and x^-_a, are introduced in M^+ and M^-. For any tensor A_{ab}, with at most a simple discontinuity at Σ,

$$[A_{ab}]^{\sim}(P)\equiv \lim_{Q\to P^+} A^+_{ab}(Q)-\lim_{R\to P^-} A^-_{ab}(R)$$

and

$$[A_{ab}]^{\wedge}(P)\equiv \left[\lim_{Q\to P^+} A^-_{ab}(Q)+\lim_{R\to P^-} A^-_{ab}(R)\right]/2$$

are the jump and mean value, respectively, where $P^+\in\Sigma^+$, $P^-\in\Sigma^-$, and $Q\to P^+,R\to P^-$ through M^+,M^-, respectively. The above expressions will only be meaningful and in particular, will transform correctly in a tensorial way if there exists a mapping $\mathscr{M}:\Sigma^+\to\Sigma^-$ whose derivatives will in the usual way relate components relative to the two coordinate systems in the surface Σ, i.e., $P^+\to P^-$. The condition of continuity of the metric can be stated then as $[g_{ab}]^{\sim}=0$.

The three-metric intrinsic to the timelike hypersurface Σ is given by

$$h_{ab}=g_{ab}-n_a n_b \ , \tag{2.1}$$

where n_a is the unit normal to Σ directed from M^- to M^+, n_a is everywhere spacelike ($n^a n_a=+1$), and $h^a_b=g^{ac}h_{cb}$ is a projection operator into the subspace Σ. As usual, the metric g_{ab} defines a connection on M, and we will denote covariant differentiation with respect to this connection by (;). In a similar way, the induced metric h_{ab} on Σ defines a connection; covariant differentiation with respect to this connection will be denoted by (|).

The second fundamental form of Σ or extrinsic curvature K_{ab} of Σ is then defined by

$$K_{ab}\equiv n_{a\,|\,b}=K_{ba} \ , \tag{2.2}$$

where the sign of K_{ab} is in agreement with the convention employed by Israel,[8] but opposite to the convention of Misner, Thorne, and Wheeler.[10]

In terms of the intrinsic and extrinsic curvatures of Σ, the Einstein tensor has components

$$G_{ab}n^a n^b=-({}^3R+K_{ab}K^{ab}-K^2)/2 \ , \tag{2.3a}$$

$$G_{bc}h^b_a n^c=K^b_{a\,|\,b}-K_{|\,a} \ , \tag{2.3b}$$

$$\begin{aligned}G_{cd}h^c_a h^d_b={}^3G_{ab}&-(K_{cd}-h_{cd}K)^* h^c_a h^d_b-KK_{ab}\\&+(K^2+K_{cd}K^{cd})h_{ab}/2-n^*_a n^*_b\\&+n^*_{(a\,|\,b)}-h_{ab}(n^{c*})_{;c} \ ,\end{aligned} \tag{2.3c}$$

where ${}^3R$ and ${}^3G_{ab}$ are the Ricci scalar and Einstein tensor of the three-geometry h_{ab} of Σ, respectively, with $K\equiv K^a_a$ and $(\ )^*\equiv(\ )_{;a}n^a$. Equations (2.3a) and (2.3b) are the so-called contracted Gauss-Codazzi equations.

B. Discontinuity behavior

Although it was assumed that the metric g_{ab} contains no jump discontinuity or δ-function singularity, the extrinsic curvature K_{ab} may have a singularity. Since K_{ab} is roughly the normal derivative of the metric, δ-function singularities in K_{ab} correspond to discontinuities of the metric and therefore are excluded here. However jump discontinuities in K_{ab}, corresponding to "ramps" in the metric, are possible. This implies that the Einstein tensor (2.3) (second derivatives of the metric), and so the energy-momentum tensor T_{ab} on M, can have a jump discontinuity and/or a δ-function singularity due to a possible jump discontinuity of the extrinsic curvature K_{ab}.

C. δ-function behavior

To discover the effect of the stress-energy tensor S_{ab} of Σ on the space-time geometry, one must perform a "pill-box" integration of Einstein's equations $G_{ab}=8\pi T_{ab}-\Lambda g_{ab}$ across Σ:

$$S_{ab}\equiv\lim_{\Sigma\to 0}\int_{-\Sigma}^{\Sigma}[T_{ab}-g_{ab}\Lambda/8\pi]dn$$
$$=(1/8\pi)\lim_{\Sigma\to 0}\int_{-\Sigma}^{\Sigma}G_{ab}dn\ , \tag{2.4}$$

where n is the proper distance through Σ in the direction of the normal n_a. In the absence of δ functions and jump discontinuities in g_{ab}, and of δ functions in K_{ab}, the Einstein tensor (2.3) when integrated yields

$$\lim_{\Sigma\to 0}\int_{-\Sigma}^{\Sigma}G_{ab}n^an^bdn=0=8\pi S_{ab}n^an^b\ , \tag{2.5a}$$
$$\lim_{\Sigma\to 0}\int_{-\Sigma}^{\Sigma}G_{cb}n^bh_a^cdn=0=8\pi S_{cb}n^bh_a^c\ , \tag{2.5b}$$
$$\lim_{\Sigma\to 0}\int_{-\Sigma}^{\Sigma}G_{cd}h_a^ch_b^ddn=-(K_{ab}-h_{ab}K)^{\sim}$$
$$=8\pi S_{cd}h_a^ch_b^d\ , \tag{2.5c}$$

where the last and only nonvanishing equation gives the jump of the extrinsic curvature across Σ; Eqs. (2.5a) and (2.5b) have the physical meaning that no momentum associated with the surface layer flows out of Σ.

Attention will be restricted to perfect-fluid gravitational sources, so that on Σ, the stress-energy tensor is given by

$$g^{ab}=\sigma u^au^b-\tau(h^{ab}+u^au^b) \tag{2.6a}$$

and off the hypersurface by

$$T^{ab}=\mu v^av^b+p(g^{ab}+v^av^b)\ , \tag{2.6b}$$

where u^a is the four-velocity of any observer whose world line lies within Σ and sees no energy flux in his local frame; σ and τ, are respectively, the surface-energy density and tension measured by that observer. Similarly, v^a is the four-velocity of any observer in M who sees no energy flux in this local frame, with μ and p the energy density and pressure measured by v^a.

From Eqs. (2.5a) and (2.5b) it follows that the structure (2.6a) assumed for S_{ab} is allowable. The remaining equations (2.5c) are the so-called Lanczos equations, which can be rewritten as

$$\tilde{K}_{ab}=-8\pi(S_{ab}-h_{ab}S/2)\ . \tag{2.7}$$

D. Jump behavior

Since the "pill-box" integration (2.5) ignores a simple jump discontinuity, a jump analysis, which ignores any delta behavior, is needed. This analysis of Einstein's equations (2.3) consists of taking left and right limits as one approaches the layer Σ. This limit process applied in the regions M^+ and M^- to the contracted Gauss-Codazzi equations (2.3a) and (2.3b) restricts the jumps of the gravitational quantities and subjects the extrinsic curvature to eight conditions:

$$G_{ab}^{\pm}n_{\pm}^an_{\pm}^b=-\tfrac{1}{2}({}^3R+K_{ab}^{\pm}K_{\pm}^{ab}-K_{\pm}^2)\ ,$$
$$G_c^{\pm}h_a^bn_{\pm}^c=K_{a\,|b\pm}^{b}-K_{|a\pm}\ .$$

The sum and difference of the corresponding pairs of these equations give, with the help of Lanczos equations (2.7), an equivalent set of conditions called "jump conditions":[8]

$$S_{a\,|b}^b=-[T_{bc}n^ch_a^b]^{\sim}\ , \tag{2.8a}$$
$$\hat{K}_{ab}S^{ab}=[T_{ab}n^an^b-\Lambda/8\pi]^{\sim}\ , \tag{2.8b}$$
$$\hat{K}_{a\,|b}^{b}-\hat{K}_{|a}=8\pi[T_{bc}n^ch_a^b]^{\wedge}\ , \tag{2.8c}$$
$${}^3R+(\hat{K}_{ab}\hat{K}^{ab}-\hat{K}^2)=-16\pi[T_{ab}n^an^b-\Lambda/8\pi]^{\wedge}$$
$$-16\pi^2(S^{ab}S_{ab}-S^2/2)\ . \tag{2.8d}$$

These jump conditions have the form of intrinsic tensor equations and consequently do not depend on the way in which the coordinate charts x^{a+} and x^{a-} are introduced in M^+ and M^-. On writing these equations, it is assumed that the mapping $\mathscr{M}:\Sigma^+\to\Sigma^-$ exists in order to guarantee that the evaluation of such tensorial quantities can be made in some standard frame at the same point. These equations, together with Lanczos equations, represent the fundamental set of boundary conditions for the gravitational field on the hypersurface Σ.

Equation (2.8a) expresses the energy-momentum balance of matter in the hypersurface; in other words, it describes how the gravitational field in the neighborhood of Σ may transfer energy and momentum to the matter in the hypersurface. The influence of the surface distribution of matter S_{ab} and of the mean values of $T_{ab}n^an^b$ and $T_{bc}n^bh_a^c$ on the intrinsic curvature ${}^3R$ and the mean extrinsic curvature K_{ab} of the hypersurface Σ is expressed by the jump conditions (2.8c) and (2.8d).

Finally, Eq. (2.8b) and Lanczos equations (2.7) can be rewritten, by means of the definition (2.2), as

$$[n^aS_{a;b}^b]^{\wedge}=-[T_{ab}n^an^b-\Lambda/8\pi]^{\sim} \tag{2.9a}$$

and

$$[n^aS_{a;b}^b]^{\sim}=8\pi(S^{ab}S_{ab}-S^2/2)\ , \tag{2.9b}$$

respectively. These equations express the normal force acting on the respective sides of an element of the hypersurface Σ as a consequence of the self-interaction in the element [see (2.9b)] and of the energy momentum transferred from the media on $M^\pm$ to Σ [see (2.9a)].

E. The general equations

What has been done up to this point is to use Israel's formalism to write the set of equations, Lanczos equations (2.7) and jump conditions (2.8), equivalent to Einstein's equations in the vicinity of a hypersurface of discontinuity. In addition to these equations, one also has to include Einstein's field equations and contracted Bianchi identities off the hypersurface with a suitable description of matter on Σ and $M^\pm$ (2.6). Continuity of the metric g_{ab} across the hypersurface Σ completes the set of general equations to solve Einstein's equations in a manifold M containing a surface of discontinuity.

As expected from other situations, this set of equations as stated above cannot completely determine a solution. Equations of state must be provided for the fluid in $M^\pm$ and Σ. However, for the case that will be analyzed in Sec.

IV, the assumption that both $M^{\pm}$ are spatially flat FRW space-times does not allow for provision of arbitrary equations of state in both M^+ and M^- at the same time because the system of equations with this symmetry becomes overdetermined. Consequently, one equation of state is not given and will be obtained by the matching.

Summarizing, the following set forms the general equations to solve Einstein's equations in the presence of a hypersurface of discontinuity: (1) Einstein's equations and contracted Bianchi identities off Σ; (2) Lanczos equations (2.7); (3) jump conditions (2.8); (4) continuity of the metric g_{ab} across Σ; (5) description of matter on Σ and $M^{\pm}$ (2.6); (6) equations of state.

Our analysis based on these equations has two main objectives: We will investigate the history of the hypersurface Σ, and we will find the mapping $\mathscr{M}:\Sigma^+\to\Sigma^-$ that effects the matching across Σ for the case of thin spherical shells.

III. THIN SPHERICAL SHELLS

Until now nothing has been said about the hypersurface's symmetry. In this section we shall apply the formalism of the previous section to spherically symmetric surfaces of discontinuity, and we shall study thin shells (bubbles) immersed in Schwarzschild de Sitter space-times. In particular, vacuum bubbles that nucleate in phase transitions in the very early Universe are studied under the assumption that they possess a domain-wall structure. The mapping $\mathscr{M}:\Sigma^+\to\Sigma^-$ is found explicitly in terms of the coordinates in the Lemaitre-Robertson frame, which allow us to extend beyond the de Sitter event horizon.

A. Bubbles

Because of the symmetry, the metric in the region $M^+(M^-)$ outside (inside) the bubble's wall Σ can be represented by a nonstatic spherically symmetric perfect-fluid solution of Einstein's field equations. In a comoving frame of reference, the line element may be written as[11]

$$ds^2|_{\pm}=-\exp(2\nu)dt^2+\exp(2\lambda)dr^2+Y^2d\Omega^2|_{\pm}\ , \tag{3.1}$$

where $\nu=\nu(r,t)$, $\lambda=\lambda(r,t)$, $Y=Y(r,t)$, $d\Omega=d\theta^2+\sin^2\theta\times d\phi^2$, and $v^3=(e^{-\nu},0,0,0)$ is the four-velocity of an element of the medium.

The symmetry of the problem also allows us to choose the coordinates θ and ϕ continuous across Σ, but in general, the time and radial coordinates are not continuous on the wall. In fact, two conditions on these coordinates can be obtained if we impose the continuity of the metric, which tells us that distances measured on Σ^+ and Σ^- must agree.

Let l be the proper time along timelike streamlines ($\theta,\phi=$const) of an observer whose world line lies within Σ and $r^{\pm}|_{\Sigma^{\pm}}\equiv R^{\pm}$ be the coordinate radius of the bubble, then comparison of timelike lines ($\phi,\theta=$const) on Σ^+ and Σ^- yields

$$[-\dot t^{\,2}\exp[2\nu(R,t)]+\dot R^{\,2}\exp[2\lambda(R,t)]]^{\sim}=0\ , \tag{3.2a}$$

and the identification of two-spheres ($R^{\pm},t^{\pm}=$const) on Σ^+ and Σ^- leads to

$$[Y(R,t)]^{\sim}=0\ , \tag{3.2b}$$

where $(\ )^{\cdot}\equiv(\ )_{;a}u^a\equiv d/dl$ is the proper-time derivative. Condition (3.2b) has the physical interpretation that observers in M^+ and M^- must measure the same value for the physical radius of the bubble.

The tangent vector to any point in the bubble wall is given by

$$u^a_{\pm}=\dot x^{\,a}_{\pm}=(\dot t,\dot R,0,0)\,|_{\pm}\ , \tag{3.3a}$$

and the normalization condition $u^{\pm}_a u^a_{\pm}=-1$ yields

$$-\dot t^{\,2}\exp[2\nu(R,t)]+\dot R^{\,2}\exp[2\lambda(R,t)]\,|_{\pm}=-1\ , \tag{3.3b}$$

which preempts Eq. (3.2a).

The unit length spatial normal $n^{\pm}_a$ is found to be, from $n^{\pm}_a u^a_{\pm}=0$,

$$n^{\pm}_a=\epsilon(-\dot R,\dot t,0,0)\exp(\nu+\lambda)\,|_{\pm}\ , \tag{3.3c}$$

where $\epsilon=+1$ if the radii of the two-dimensional spheres are growing in the direction of the outgoing normal and $\epsilon=-1$ in the opposite case.

The metric (3.1), the tangent vector $u^a_{\pm}$ (3.3a), and the normal $n^{\pm}_a$ (3.3c) allow us to rewrite the Lanczos equations (2.7) as

$$[n_a\dot u^{\,a}]^{\sim}=-4\pi(2\tau-\sigma)\ , \tag{3.4a}$$

$$\tilde K^{\theta}_{\ \theta}=-4\pi\sigma\ , \tag{3.4b}$$

and the jump conditions (2.8) as

$$\dot\sigma+2(\sigma-\tau)\dot Y/Y=[T_{ab}n^a u^b]^{\sim}\ , \tag{3.5a}$$

$$[n_a\dot u^{\,a}]^{\wedge}\sigma+2\tau\hat K^{\theta}_{\ \theta}=-[T_{ab}n^a n^b-\Lambda/8\pi]^{\sim}\ , \tag{3.5b}$$

$$[(\hat K^{\theta}_{\ \theta}Y)^{\cdot}-(n_a\dot u^{\,a})^{\wedge}\dot Y]/Y=-4\pi[T_{ab}n^a u^b]^{\wedge}\ , \tag{3.5c}$$

$$\begin{aligned}{}^3R-2\hat K^{\theta}_{\ \theta}[\hat K^{\theta}_{\ \theta}+2(n_a\dot u^{\,a})^{\wedge}]\\ =-16\pi[T_{ab}n^a n^b-\Lambda/8\pi]^{\wedge}-8\pi^2\sigma(\sigma-4\tau)\ ,\end{aligned} \tag{3.5d}$$

where

$$K^{\theta}_{\ \theta}=\epsilon(Y_{,t}\dot R e^{\lambda-\nu}+Y_{,R}\dot t e^{\nu-\lambda})/Y\ ,$$

$$n_a\dot u^{\,a}=\epsilon(\ddot R+\dot\lambda\dot R+\dot t^{\,2}\nu_{,R}e^{2(\nu-\lambda)}+\dot R\dot t\lambda_{,t})e^{\lambda-\nu}/\dot t\ ,$$

where $(\ )_{,t}\equiv\partial/\partial t$ and $(\ )_{,R}\equiv\partial/\partial R$.

Equation (3.5a) shows clearly the energy-momentum balance in the bubble's wall; this equation, together with the equation of motion, determines completely the history of the bubble. The Lanczos equation (3.4b) yields directly the equation of motion for the shell

$$\dot Y^{\,2}=(Y\tilde\eta/2M)^2+(M/2Y)^2-\hat\eta\ , \tag{3.6}$$

where $M\equiv4\pi Y^2\sigma$ and $\eta\equiv(Y_{,R}e^{-\lambda})^2-(Y_{,t}e^{-\mu})^2$. Lake showed[3] that this equation of motion can be derived without the explicit form of the stress-energy momentum S_{ab} on Σ.

B. Vacuum bubbles

With the introduction of the "inflationary scenario" of early cosmology, proposed by Guth,[1] there have been recently several investigations of bubbles in vacuum phase transitions,[4,7,12,13] where these bubbles are immersed in a de Sitter geometry.

The interest in vacuum bubbles began with the work of Coleman,[14] and later Coleman and De Lucia.[2] They showed that it is possible for a classical field theory to have two stable homogeneous ground states, only one of which is an absolute energy minimum. In the quantum version of the theory, the ground state of higher energy is a false vacuum, rendered unstable by barrier penetration.

The decay of false vacuum is initiated by the materialization of a bubble of true vacuum, with vacuum energy $\Lambda^-/8\pi$, within the false vacuum of energy $\Lambda^+/8\pi$, $(\Lambda^+ \geq \Lambda^-)$. In order to apply the formalism developed by Israel to these bubbles, one has necessarily to assume the thin-wall approximation; Coleman[14] showed that this approximation is only valid if the potential difference between the real and false vacuum is much smaller than the potential barrier between them, which is the case in the "old inflationary scenario."[1] There are, however, a number of cases where this approximation turns out to be a crude one; in particular, it is inapplicable to the "new inflationary scenario."[9]

Assuming that the thin-wall approximation is valid, we find the equations (earlier obtained by Berezin, Kuzmin, and Tkachev[4]) that determine the history of a bubble immersed in a Schwarzschild de Sitter space-time. In particular we obtain, for bubbles with vanishing Schwarzschild parameter and domain-wall structure (vacuum bubbles), the mapping $\mathscr{M}:\Sigma^+ \to \Sigma^-$ that effects the matching in the bubble wall Σ of the two submanifolds M^+ (exterior), M^- (interior). We start with a de Sitter metric written in the static frame; this frame suffers a coordinate singularity at the de Sitter event horizon; therefore, we will eventually give a coordinate transformation to the Lemaitre-Robertson frame which allows an analytical continuation of the mapping $\mathscr{M}$ beyond that event horizon.

Because of the symmetry and vacuum nature of the problem, the metric is in the exterior region M^+ Schwarzschild de Sitter and in the interior region M^- de Sitter, i.e.,

$$ds^2|_{\pm} = -f(r)dt^2 + f^{-1}(r)dr^2 + r^2 d\Omega^2|_{\pm} , \tag{3.7}$$

where $f^+(r_+) \equiv 1 - 2m/r_+ - \Lambda^+ r_+{}^2/3$ and $f^-(r_-) \equiv 1 - \Lambda_- r_-{}^2/3$, with m the Schwarzschild parameter.

In writing the jump conditions (3.5), we showed explicitly the cosmological term; consequently, the energy-conservation equation (3.5a) with $T^{\pm}_{ab}=0$ (vacuum decay) takes the form

$$\dot{\sigma} + 2(\sigma - \tau)\dot{Y}/Y = 0 . \tag{3.8}$$

From this equation, it is clear that as the bubble expands there is no vacuum energy transferred to the surface energy of the bubble from $M^{\pm}$ regions since $[\Lambda g_{ab} n^a u^b]^{\sim} = 0$. The liberated vacuum energy is completely transformed into kinetic energy of the shell. Substitution of the metric (3.7) into the equation of motion (3.6) yields

$$\dot{R}^2 = (R/R_0)^2 - 1 + [1 + \tilde{\Lambda}/48(\pi\sigma)^2]m/R + (m/4\pi\sigma F^2)^2 , \tag{3.9}$$

where

$$R_0{}^2 = (3\sigma)^2[(\hat{\Lambda}/4\pi + 6\pi\sigma^2)^2 - (\Lambda^+\Lambda^-)/16\pi]^{-1}$$

and

$$m = -\tilde{\Lambda}R^3/6 + 4\pi\sigma R^2(\dot{R}^2 + 1 - \Lambda^- R^2/3)^{1/2} - 8\pi^2\sigma^2 R^3 .$$

Equation (3.9) shows that the kinetic energy of the wall increases as it expands from its minimum radius R_0. No distinction is made in the bubble's radius $R^{\pm}$ since in the chosen coordinates the continuity of the metric (3.2b) yields $Y \equiv R^+ = R^-$; i.e., the coordinate and physical radius of the bubble are the same.

Given the equation of state for the wall, the history of the bubble is completely determined by Eqs. (3.8) and (3.9). The remaining equations, Lanczos equation (3.4a), and jump conditions (3.5b)–(3.5d) either hold identically or can be derived from (3.8) and (3.9).

It has been shown[15] that the phase separation for vacuum phase transitions has a domain-wall structure; surface energy density σ equals its tension τ. Then from the energy-conservation equation (3.8) the surface energy density, and consequently its tension, must be constant. Even with this simplification, to our knowledge there are no analytical general solutions to the equation of motion (3.9). However, since in the process of vacuum decay the bubble appears spontaneously as a new vacuum bubble created during the phase transition, it should not affect the geometry outside Σ; i.e., the Schwarzschild parameter m must vanish. It follows then from (3.9) that

$$\dot{R}^2 = (R/R_0)^2 - 1 ,$$

which is the case of vacuum bubbles expanding according to the de Sitter law

$$R(l) = R_0 \cosh(l/R_0) . \tag{3.10}$$

We identify the nucleation time of the bubble as the time t_0^+ (t_0^-) when R achieves its minimum, $R = R_0$; the proper time in the bubble is set to zero at that instant. As we said before, we are not only interested in the history of the bubble's wall Σ, but also in the mapping $\mathscr{M}:\Sigma^+ \to \Sigma^-$ that effects the matching across the hypersurface. We will restrict ourselves, for the sake of simplicity, to bubbles in which the true vacuum energy $\Lambda^-/8\pi$ vanishes; i.e., the space-time M^- in the interior of the bubble is Minkowski. This could be the case of bubbles in the old inflationary universe scenario.

With the help of the normalization condition (3.3b), the equation of the coordinate radius (3.10), can be rewritten as

$$R^2 - (1 - H^2 R_0{}^2)H^{-2}\tanh^2[H(t^+ - t_0^+)] = R_0{}^2 \tag{3.11a}$$

in M^+ (de Sitter), and

$$R^2 - (t^- - t_0^-)^2 = R_0{}^2 \tag{3.11b}$$

in M^- (Minkowski), where $\Lambda^+ \equiv 3H^2$ and R_0

$=\sigma(2\pi\sigma^2+\Lambda^+/24\pi)^{-1}$ is the initial radius of the bubble.

Although the above expressions give directly the mapping $\mathscr{M}$, they involve two related nondesirable points. First, Eq. (3.11a) is able to describe the evolution of the bubble only for radius R smaller than the de Sitter event horizon H^{-1}, and, second, the time coordinate t^+ is not cosmic time; both problems arise from choosing to start with coordinates in the static frame for the metric (3.7), which describe the space-time for values of the coordinate r smaller than the event horizon $(3/\Lambda^{\pm})^{1/2}$. We then go to the Lemaitre-Robertson frame where the de Sitter metric appears spatially flat:

$$ds^2|_+=-dT^2+e^{2HT}(d\rho^2+\rho^2 d\Omega^2)\ . \tag{3.12}$$

In these coordinates, Eq. (3.11a) reads

$$F^2e^{2HT}-(1-H^2R_0{}^2)H^{-2}\tanh^2\{H(T-T_0) - \tfrac{1}{2}\ln[(1-H^2F^2e^{2HT})/(1-H^2R_0{}^2)]\}=R_0{}^2\ ,$$

where $\rho|_\Sigma\equiv F$ is the coordinate radius of the bubble, and T_0 is the cosmic time when the bubble was nucleated; the physical radius of the bubble is given now by Fe^{HT}. A straightforward calculation, using the continuity conditions (3.2) on the above equation, leads to the explicit form of the mapping $\mathscr{M}$ as

$$H(T-T_0)=\ln[1+H(t^- - t_0^-)/(1-H^2R_0{}^2)^{1/2}]\ , \tag{3.13a}$$

for $T\mapsto t^-$, time coordinate mapping, and

$$F=Re^{-HT_0}[1+H(R^2-R_0{}^2)^{1/2}/(1-H^2R_0{}^2)^{1/2}]^{-1}\ , \tag{3.13b}$$

For $F\mapsto R$, coordinate radius mapping. Implicit in these equations is the assumption that the initial radius of the bubble R_0 is smaller than H^{-1}.

Even though we started from expressions (3.11), which suffer from the coordinate singularity at H^{-1} (Fig. 1), the mapping (3.13) has been written in coordinates which are free of such singularity, and, therefore, it is possible analytically to continue these solutions to regions where the coordinate radius of the bubble is larger than the event horizon of the de Sitter space-time. That is, the history of the bubble $[R(l)$, l the proper time$]$ is unaffected by the defect of the t^+ coordinate in the neighborhood of the horizon.

Since the expansion of the bubble is already described by Eq. (3.10), the main interest of Eqs. (3.13) for $\mathscr{M}$ is explicitly to see how the time and radial coordinate are identified in the bubble wall. In this case we see that the joining of M^+ with M^- is possible for any value of the bubble radius; however, as we shall see in Sec. IV, it is not always possible in other situations to carry out this procedure.

Finally, in order to have a schematic picture of the bubble's growth viewed from M^+, we will rewrite the equation of the coordinate radius (3.11a) in terms of the coordinates (v,w,x,y,z), where the de Sitter metric takes the five-dimensional Minkowski form $ds^2=-dv^2+dw^2+dx^2+dy^2+dz^2$; in these coordinates, the de

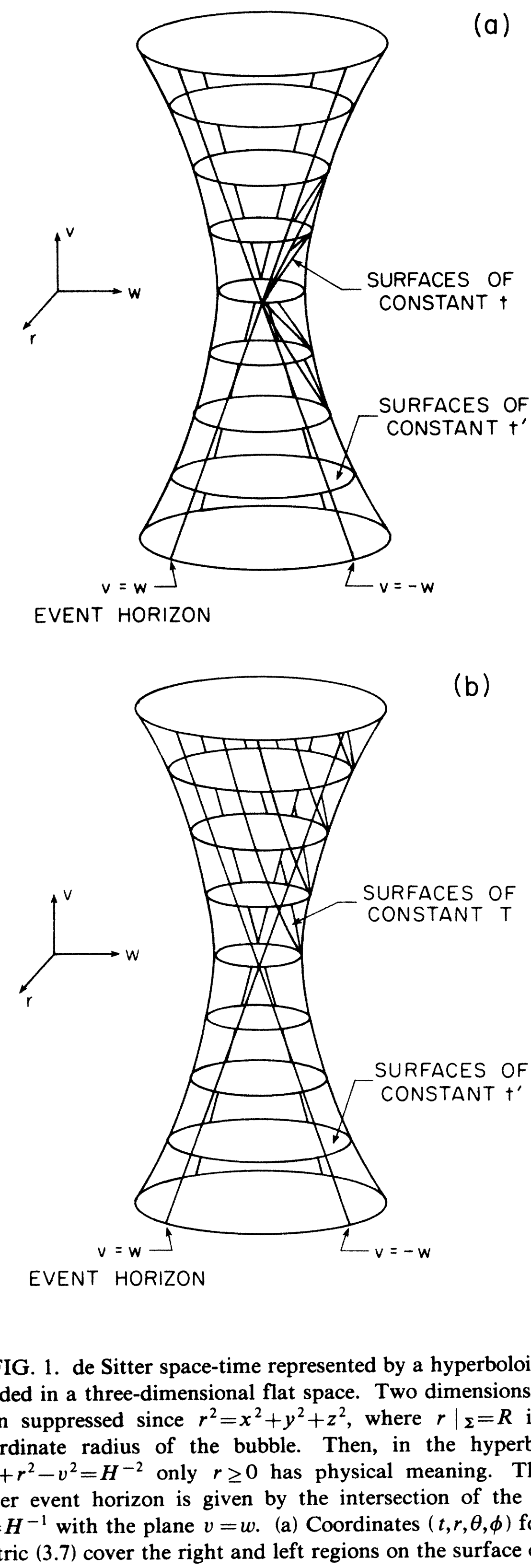

FIG. 1. de Sitter space-time represented by a hyperboloid imbedded in a three-dimensional flat space. Two dimensions have been suppressed since $r^2=x^2+y^2+z^2$, where $r|_\Sigma=R$ is the coordinate radius of the bubble. Then, in the hyperboloid $w^2+r^2-v^2=H^{-2}$ only $r\geq 0$ has physical meaning. The de Sitter event horizon is given by the intersection of the plane $r=H^{-1}$ with the plane $v=w$. (a) Coordinates (t,r,θ,ϕ) for the metric (3.7) cover the right and left regions on the surface of the hyperboloid that lie between the planes $v=w$ and $v=-w$; i.e., they do not describe the region beyond the event horizon. (b) Coordinates (T,ρ,θ,ϕ) in (3.12) cover the surface above the plane $w=-v$. Finally, coordinates (t',χ,θ,ϕ), in which the metric takes the form $ds^2=-dt'^2+H^{-2}\cosh^2(Ht')\times(d\chi^2+\sin^2\chi\, d\Omega^2)$, cover the whole hyperboloid.

Sitter space-time is visualized as the hyperboloid $-v^2+w^2+x^2+y^2+z^2=H^{-2}$ (Ref. 16). Choosing $t_0^{\pm}=T_0=0$, Eq. (3.11a) now becomes

$$R^2-w_0^2(v/w)^2=R_0^2\ , \tag{3.14}$$

where $x^2+y^2+z^2|_\Sigma=r^2|_\Sigma\equiv R^2$, $v_0=0$, and $w_0=H^{-1}(1-H^2R_0^2)^{1/2}$. Substitution of this equation into the hyperboloid where the bubble lies, $(w^2-v^2)H^2=1-H^2R^2$, yields

$$R^2-v^2=R_0^2 \tag{3.15a}$$

and

$$w=H^{-1}(1-H^2R_0^2)^{1/2}=\text{const}\ . \tag{3.15b}$$

That is, the radius of the bubble has a hyperbolic growth (3.15a) on the plane defined by (3.15b), see Fig. 2. In particular, if one considers the limit case of a bubble nucleated with a vanishing radius, the trajectory on the plane $w=H^{-1}$ is a straight line $R=v$.

Finally, we mention that Aurilia, Denardo, Legovini, and Spallucci[17] have also suggested that the process of vacuum bubbles in the cosmological phase transitions could be interpreted in terms of a vacuum energy density analogous to that of the hadronic phase in the physics of strong interactions. Their approach to bubble dynamics is based on a general theory of relativistic extended objects; in particular, the radial equation (3.9) is obtained from an action functional that involves a three-index potential which mediates the interaction between the hypersurface elements along the world tube of a bubble. Recently, a more detailed study of evolution of bubbles in a vacuum has been completed by Lake and Wevrick.[18] Their work involves an extensive analysis of spherical bubbles in a vacuum under the assumption that the intrinsic surface tension and energy density are proportional.

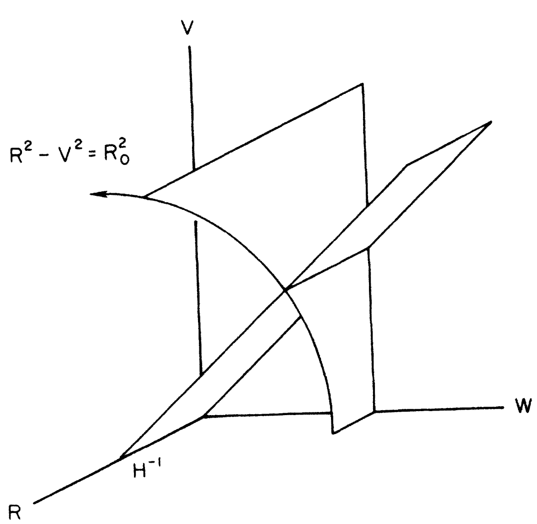

FIG. 2. Growth of the bubble on the de Sitter hyperboloid $R^2+w^2-v^2=H^{-2}$. In the chosen coordinates only positive values of R are allowed. To avoid confusion, the surface of the hyperboloid has been suppressed; only the planes of the event horizon $w=v$ and of the bubble radius $w=H^{-1}(1-H^2R_0^2)^{1/2}$ were drawn.

IV. BUBBLES IN FRW SPACE-TIME

In the problem of phase separation boundaries, besides the common picture of a shell separating two phases with pure vacuum equations of state as we considered in Sec. III, there are several studies without a full inclusion of gravitational effects,[12,13,19] which suggest the rise of bubbles in phase transitions in the early Universe could have been similar to the process of motion of spherical detonation waves. That is, contrary to the case of vacuum bubbles studied in Sec. II B, as the bubble expands the the entire energy of the metastable vacuum is transformed into the energy of the internal medium. Consequently, the energy and momentum are conserved across the bubble's wall, which leads to a vanishing surface density density but, in general, to a nonvanishing tension. The work against tension determines the kinetic energy of the bubble's wall (and thus the rate of vacuum energy transformed into energy of the internal medium).

A generalization of this model including gravitational effects, which to some extent admits analytical solution, is to analyze a bubble immersed in a spatially flat Friedmann-Robertson-Walker (FRW) space-time. In particular we shall consider models which are FRW on both sides of the shell. Also, it will be assumed that the medium in M^- is a radiation field with $\Lambda^-/8\pi=0$. The medium in M^+ has a nonvanishing vacuum energy $\Lambda^+/8\pi$ in addition to a matter content, whose equation of state will be determined by the matching.

First, the general equations discussed in Sec. II E are rewritten explicitly in terms of the metric in $M^{\pm}$. It is found that if we give only the parameters of M^-, the system is underdetermined, so additional assumptions must be made. It will then be shown that the bubble here considered only admits a junction at the bubble, with M^+ and M^- spatially flat FRW submanifolds, in a wormhole fashion. That is, the submanifolds M^+ and M^- are the infinite-extent exteriors of a sphere; matching of the interiors (anti-worm holes) is also possible. Finally, the evolution of such a "bubble" is obtained in the particular cases when the wall Σ follows a Hubble law and when the tension in the shell is constant.

The metric in $M^{\pm}$ can be written as

$$ds^2|_{\pm}=-dt^2+a^2(t)(dr^2+r^2d\Omega^2)|_{\pm}\ , \tag{4.1}$$

and the induced metric on the surface of the bubble is $ds^2|_\Sigma=-dl^2+Y^2(l)d\Omega^2$, where $Y\equiv aR\,|_{\pm}$ is the radius of the bubble and $r\,|_\Sigma\equiv R$ its coordinate radius.

The general equations (Sec. II E) that describe the problem can now be written in terms of the coordinates (4.1). First, since M^+ and M^- are FRW space-time manifolds, the contracted Bianchi identities and Einstein's equations off the wall Σ yield

$$\mu_{,t}=-3(\mu+p)a_{,t}a^{-1} \tag{4.2a}$$

and

$$3a_{,t}{}^2=(8\pi\mu+\Lambda)a^2\ , \tag{4.2b}$$

respectively. However, we will pose the expansion and the fluid parameters in only one of the two regions because the matching will determine the parameters of the other submanifold. Complete specification of both M^+ and M^- overdetermines the system of equations. This case differs from the previous one in Sec. III, where a complete description of M^+ and M^- was given and the only parameters that remained to be found were those of the shell.

The continuity condition of the metric (3.2b), which says that observers in M^+ and M^- must measure the same radius for the bubble, can be restated as

$$Y \equiv a^- R^- = a^+ R^+ \ . \tag{4.3a}$$

The normalization condition (3.3b) evaluated in Σ^+ and Σ^- gives another two equations:

$$(1-H^2Y^2)\dot t = -HY\dot Y + \beta(\dot Y^2 + 1 - H^2Y^2)^{1/2}\,|_{\pm} \ , \tag{4.3b}$$

where $\beta = \pm 1$ takes care of the two possible solutions for $\dot t$ in (3.3b).

It can be shown that for M^+ and M^- FRW spacetimes, Lanczos equation (3.4a) is not independent of (3.4b). Substitution of (4.2b) into the square of (3.4b) yields

$$H_+{}^2 = H_-{}^2 \equiv H^2 \ , \tag{4.4a}$$

where $H \equiv a_{,t} a^{-1}$. We shall assume that $H^+ = H^- > 0$. The negative case can be obtained by reversal of the direction of time on both sides of the wall. Also from Lanczos equation (3.4b), one gets a condition that will fix the topology of the matching. See the discussion after Eq. (4.6b) below. The condition is that

$$\epsilon^+\beta^+ = \epsilon^-\beta^- \ , \tag{4.4b}$$

where the sign $\beta^\pm = \pm 1$ is defined in (4.3b) and $\epsilon^\pm = \pm 1$ is the undetermined sign of the normal n^a in (3.3c).

Finally, since the region M^- will be completely characterized, only one of the four jump conditions (3.5) is needed. For this particular case, (3.5a) and (3.5b) turn out not to be independent. Both equations lead to

$$-2\tau(1-H^2Y^2)/Y = \tilde\epsilon[(p+\mu)\dot t]^{\hat{}} \ , \tag{4.5}$$

which expresses the flux of momentum transferred to the shell.

By assumption the medium M^- is a radiation fluid without vacuum energy density, $p^- = \mu^-/3$, $8\pi\mu^-/3 = (2t^-)^{-2}$, and $a_-{}^2 = 2At^-$; i.e., the region M^- has been completely characterized. We will then proceed to find solutions for the unknowns in Σ ($R_\pm, t_\pm, \tau$) and in M^+ (p_+, μ_+, a_+). However, we still must specify one extra condition since the system of equations to this point is undetermined, eight unknowns and seven equations [(4.2a), (4.2b), (4.3a), (4.3b$^+$), (4.3b$^-$), (4.4a), and (4.5)].

Before the additional condition is introduced, we will analyze the junction conditions for the matching of manifolds M^+ and M^- on the bubble wall Σ. First, from the substitution of the continuity of the Hubble constant (4.4a) into Einstein's equation (4.2b). We obtain that the total energy density is continuous across Σ, i.e.,

$$\mu^+ + \Lambda^+/8\pi = \mu^- \ ; \tag{4.6a}$$

in addition, the equation of conservation of energy (4.2a) yields

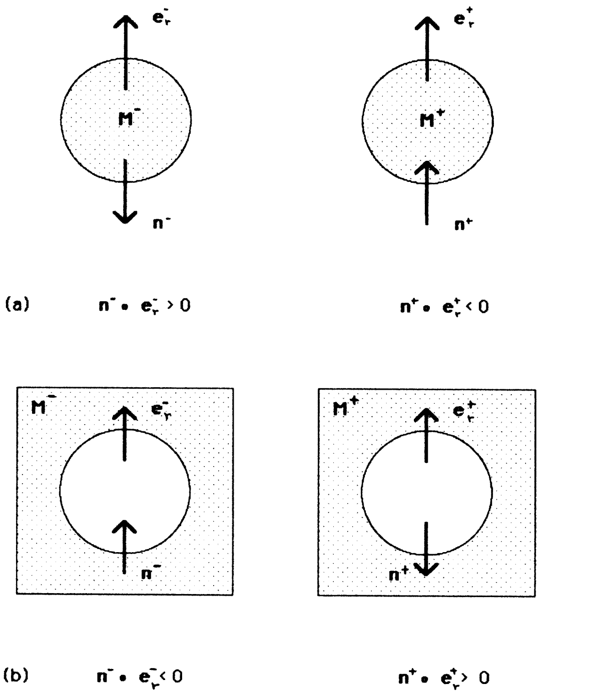

FIG. 3. The matching $\mathscr{M}:\Sigma^+ \to \Sigma^-$ for different values of $\tilde\epsilon$ Eq. (4.8). When $\tilde\epsilon = -2$, anti-worm-hole, the joining is between the interior regions (a), and when $\tilde\epsilon = +2$, worm hole, the exterior regions are identified (b).

$$(\mu+p)\dot t\,|_+ = (\mu+p)\dot t\,|_- \ . \tag{4.6b}$$

The weak-energy condition applied to the latter expression constrains $\dot t$ to be either positive or negative on both sides of the wall.

These two equations show that the flux of energy and momentum are continuous at the wall, which reflects the detonation wave approximation. On the other hand, from (4.3b) we have that the difference in structure of $\dot t^+$ and $\dot t^-$ is given by the sign of β. However, the choice $\beta^+ = \beta^-$ is not allowed because this would imply from Lanczos equation (4.4b) that $\tilde\epsilon = 0$, and consequently from the jump condition (4.5) τ would have to vanish. In such a situation there is complete contintuity, and the wall does not in fact exist. Therefore, we choose $\beta^+ \neq \beta^-$, and then from (4.4b) we arrive to the junction condition that $\hat\epsilon = 0$ ($\epsilon^+ = -\epsilon^-$). Substitution of this condition in the right-hand side of Eq. (4.5) shows that the tension in the bubble's wall depends on $[\epsilon(p+\mu)\dot t]^{\tilde{}}$, which can be interpreted as the work done on the shell when the matching has a worm-hole topology.

To see how the junction condition $\epsilon^+ = -\epsilon^-$ dictates a constraint on the matching, let us recall that $\epsilon = \pm 1$ was introduced because the normal $\mathbf{n}_\pm$ is determined up to a sign, i.e.,

$$\mathbf{n}_\pm = \epsilon(\dot R a \mathbf{e}_t + \dot t a^{-1}\mathbf{e}_r)\,|_\pm \ . \tag{4.7}$$

We also specified that the normal $\mathbf{n}_\pm$ is directed from M^- to M^+. Therefore,

$$\mathbf{n}\cdot\mathbf{e}_r\,|_\pm = \epsilon \dot t a^{-1}\,|_\pm \tag{4.8}$$

could be positive or negative depending on the identification made between M^+ and M^-. Since $a^{-1}>0$ and from Eq. (4.6b) $\dot{t}^{\pm}$ are either both positive or both negative, the condition $\epsilon^+=-\epsilon^-$ implies that the radial component of the normal changes sign across the bubble's wall Σ, and this can only be achieved if the matching of M^+ and M^- is made in a worm-hole fashion. That is, let us consider the problem as purely the identification of two disjoint manifolds $M^{\pm}$ and let $M^{\pm}$ be either the interior or exterior to a two-sphere $\Sigma^{\pm}$ of radius Y; the bubble will then join either the exterior of Σ^+ with the exterior of Σ^- (worm-hole matching) or the interior of Σ^+ with the interior of Σ^- (anti-worm-hole matching), see Fig. 3. The latter case implies a new topology; closed universes are connected by a shell that acts as a worm hole.

We shall now obtain a complete solution to the unknowns (p^+, a^+, μ^+, $R^{\pm}$, $t^{\pm}$, and σ) by providing an additional condition to the system of Eqs. (4.3a), (4.3b$^{\pm}$), (4.4a)–(4.6b). We will present two cases: The first allows analytical discussion; the second will be treated numerically.

We will first assume that the expansion of the bubble is governed by a Hubble law $\dot{Y}=HY$, which, together with the normalization condition (4.3b), leads to

$$\dot{t}_{\pm}=(\beta-\dot{Y}^2)/(1-Y^2)\,|_{\pm}\,. \tag{4.9}$$

For simplicity we will assume that the bubble is comoving with the radiation fluid in M^-, i.e., $\beta^-=+1$. This implies that the coordinate radius of the bubble R^- is constant and that the physical radius of the bubble grows as $Y^2=2Bt^-$, where t^- is cosmic time in M^- and also proper time for an observer comoving with the bubble, $t^-=l+\text{const}$. The constant B will be determined later on.

Substitution of $Y^2=2Bt^-$ into Eqs. (4.9) and (4.3a) yields

$$dt^+/dt^-=(B+2t^-)/(B-2t^-) \tag{4.10a}$$

and

$$dR^+/dt^-=-2R^+/(B-2t^-)\,, \tag{4.10b}$$

respectively. These equations can be directly integrated to give

$$t^+=B\ln[B/(B-2t^-)]-t^- \tag{4.11a}$$

and

$$R^+=\pm D(B-2t^-)\,, \tag{4.11b}$$

where we have chosen the integration constant in (4.11a) such that $t^+=t^-=0$ is the time when the bubble was nucleated. D is a positive constant of integration determined by the initial data; from the condition $|dR^+/dt^+|\le 1$ we obtain that $D\le\frac{1}{2}$ (Fig. 4). The case $D=\frac{1}{2}$ implies that the bubble is nucleated with a coordinate radius velocity equal to the speed of light.

The choice of the sign in Eq. (4.11b) will be positive if $B>2t^-$ and negative otherwise. We shall see that the latter case is unphysical because it implies a violation of the weak-energy condition. Consequently, from (4.11), $B>2t^-$ restricts the bubble's growth to a maximum radius $Y=B$ in a finite cosmic (also proper) time $t^-=B/2$, but in an infinite cosmic time t^+. The Eqs. (4.11a) and (4.11b) give directly the mapping $\mathcal{M}:\Sigma^+\to\Sigma^-$.

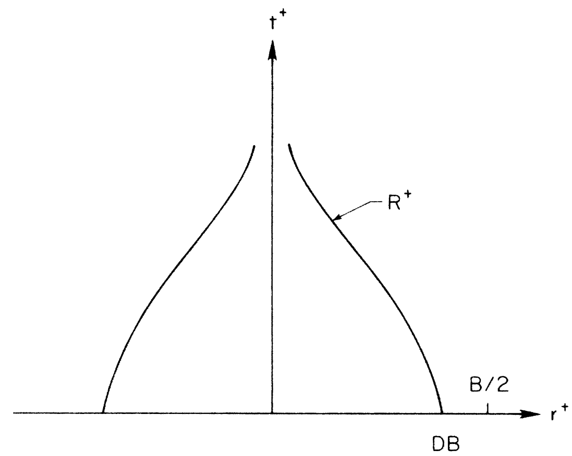

FIG. 4. The coordinate radius of the bubble viewed from M^+. For the case $\tilde{\epsilon}=+2$ the region M^+ is $r^+\ge R^+$, and for $\tilde{\epsilon}=-2$ the space-time M^+ is the closed manifold $r^+\le R^+$. Because of the condition $B\ge 2t^-$, the sign in Eq. (4.11b) is positive; the coordinate radius shrinks.

The condition $B>2t^-$ also implies that throughout its evolution the radius of the bubble, $Y^2=2Bt^-$, is larger than the event horizon distance $H^{-1}=2t^-$ in M^-. However, as the bubble grows to its maximum radius, Eq. (4.11b) shows that the coordinate radius R^+ and the velocity dR^+/dt^+ vanish; in other words, due to the great expansion in M^+, the mouth of the worm hole, viewed by a comoving observer with the fluid in M^+, disappears as $2t^-\mapsto B$. Also from (4.11b), the expansion factor in M^+ is given by

$$a^{+2}=2Bt^-(B-2t^-)^{-2}/D^2\,, \tag{4.12a}$$

which can be rewritten for $2t^-\mapsto B$ as

$$a_+{}^2=a_-{}^2e^{(2t^+/B)}/(DR^-)^2\,, \tag{4.12b}$$

and clearly $a^+\gg a^-$ for that limit.

The tension in the bubble is found from (4.5) to be

$$\tau=\tilde{\epsilon}B[4\pi(2Bt^-)^{1/2}(B-2t^-)]^{-1}\,. \tag{4.13}$$

Again, as the bubble expands, the magnitude of the tension in the wall Σ increases. Recalling that $B>2t^-$, the tension will be positive if $\tilde{\epsilon}=+2$, which is the case of a worm-hole matching, or negative if $\tilde{\epsilon}=-2$, anti-worm-hole matching (Fig. 3). Importantly, the tension tends to infinity as $2t^-\mapsto B$, so this model fails in that limit.

The difference between the pressures in M^+ and M^- is obtained from Eq. (4.6b):

$$(p_++\mu_+)=(p_-+\mu_-)(B-2t^-)/(B+2t^-)\,. \tag{4.14}$$

It is clear from this equation that $B>2t^-$ required above so the wall tension remains finite guarantees the weak-energy condition. Furthermore, as $2t^-\mapsto B$, the space-time M^+ enters a de Sitter (inflation) regime since, from

TABLE I. Schematic behavior of the physical radius of the bubble as a function of proper time $Y(l)$ and the coordinate radius as a function of cosmic time $R^-(t^-)$. For $H_0Y_0>1$, the cases ($\beta^-=+1$, $\tau/\tilde{\epsilon}<0$) and ($\beta^-=-1$, $\tau/\tilde{\epsilon}<0$) were not considered because they correspond to proper-time reversal of cases B and A, respectively. Similar for $H_0Y_0<1$, cases ($\beta^-=+1$, $\tau/\tilde{\epsilon}>0$) and ($\beta^-=-1$, $\tau/\tilde{\epsilon}>0$) are equivalent to proper-time reversal of cases D and C, respectively.

CASE	$\beta^-=\pm 1$	$\tau/\tilde{\epsilon}$	INITIAL CONDITIONS H(O), Y(O)	PHYSICAL RADIUS Y(l)	COORDINATE RADIUS $R^-(t^-)$
A	+1	>0	HY > 1	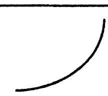	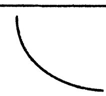
B	−1	>0	HY > 1	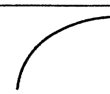	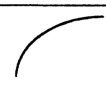
C	+1	<0	HY < 1	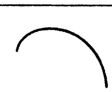	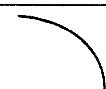
D	−1	<0	HY < 1		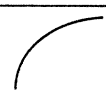

(4.12b) and (4.14), $a^+\approx\exp(t^+/B)$ and $P^+\approx-\mu^+$. Using the continuity of the total energy density (4.6a), it follows that

$$(p^+-\mu_0)-p^-=-[2t^-\pi(B+2t^-)]^{-1}<0\ . \qquad (4.15)$$

The pressure in M^+ is greater than in M^-; however, due to the special characteristic of the matching, the evolution of the bubble is governed mainly by the tension in the bubble wall.

We present now our final example. Instead of considering a bubble expanding by a Hubble law, we will change the additional assumption to be that the tension on the bubble's wall is constant. From Eq. (4.6b) and $p^-=\mu^-/3$, we find that the right-hand side of the jump condition (4.5) is given by

$$[(p+\mu)\dot{t}\,]^{\hat{}}=4\dot{t}^{\,-}\mu^-/3=H^2\dot{t}^{\,-}/2\pi=-\dot{H}/4\pi\ , \qquad (4.16)$$

which allows rewriting Eq. (4.5) as

$$\dot{H}=8\pi\tau(1-H^2Y^2)/(\tilde{\epsilon}Y)\ . \qquad (4.17)$$

On the other hand, the normalization condition (4.3b) leads to a differential equation for $\dot{Y}$ as

$$-H\dot{Y}=4\pi\tau(1-H^2Y^2)/\tilde{\epsilon}$$
$$+\beta^-\{[4\pi\tau(1-H^2Y^2)/HY\tilde{\epsilon}]^2-H^2\}^{1/2}\ , \qquad (4.18)$$

where $\beta^-=\pm1$. Here $\tilde{\epsilon}$ again determines the topology of the matching, $\tilde{\epsilon}=+2$ for a worm hole and $\tilde{\epsilon}=-2$ for an anti-worm-hole. We do not known of any analytical solution to the above system of Eqs. (4.17) and (4.18); however, before we give some numerical solutions, qualitative information can be extracted from the conditions for real solutions,

$$H^4\leq\{2\pi\tau(1-H^2Y^2)/Y\}^2\ , \qquad (4.19a)$$

and for the bubble radius to exhibit a maximum,

$$Y\leq H^{-1} \qquad (4.19b)$$

and

$$\tau\beta^-/\tilde{\epsilon}<0\ . \qquad (4.19c)$$

The first condition (4.19a) is equivalent to requiring the surface of the bubble to be a timelike hypersurface of discontinuity. Condition (4.19b) implies that a bubble which expands and then shrinks, will always have a radius smaller than the horizon distance H^{-1} in M^-. Equation (4.19c) says that the existence of such a recollapsing bubble will depend on the topology of the matching, the choice of the sign β^-, and the positive or negative nature of the tension.

The schematic behavior of the bubble radius Y as function of proper time for an observer comoving with the bubble and the coordinate radius R^- in terms of cosmic time t^- in M^- is shown in Table I. Numerical solutions to the physical radius $Y(l)$ and the coordinate radius $R^-(t^-)$ of the bubble were obtained for the cases represented in Table I when $\tau=\pm\tilde{\epsilon}/2$ and $H_0=1$ (Fig. 5). It was found that the lifetime of a bubble that glues two spatially flat FRW space-times is finite in cases A and B due to the condition for real solutions (4.19a). In case C the same restriction was present but in this case as a consequence of the condition $Y\geq0$. That is, at some point it is impossible to continue considering the tension on the surface of the bubble constant.

In addition to the case of bubbles in the vacuum (reviewed in the previous section) and the case of bubbles with vanishing surface energy density presented in this section, there have been several applications in cosmology of nonzero surface mass bubbles. One application was made (Maeda, Sato, Sasaki, and Kodama[20]) in the study of a model for late stages of the phase transition where regions of a false vacuum are surrounded by bubbles of a true vacuum. In this model an infinite number of bubbles are nucleated simultaneously on a sphere, and they grow with walls expanding isotropically at the speed of light forming a spherical shell-like region which could give rise to creation of worm holes or black holes. Another application of bubbles with nonzero surface mass is in the development of voids. Lake and Pim[21] have studied the evolution of spherical vacuum and radiation-filled voids in a spatially flat Robertson-Walker background. Similarly, Sato[22] has analyzed a model of voids which consists of a spherical thin dust shell that propagates sweeping the ambient matter and its motion is decelerated as the shell mass increases.

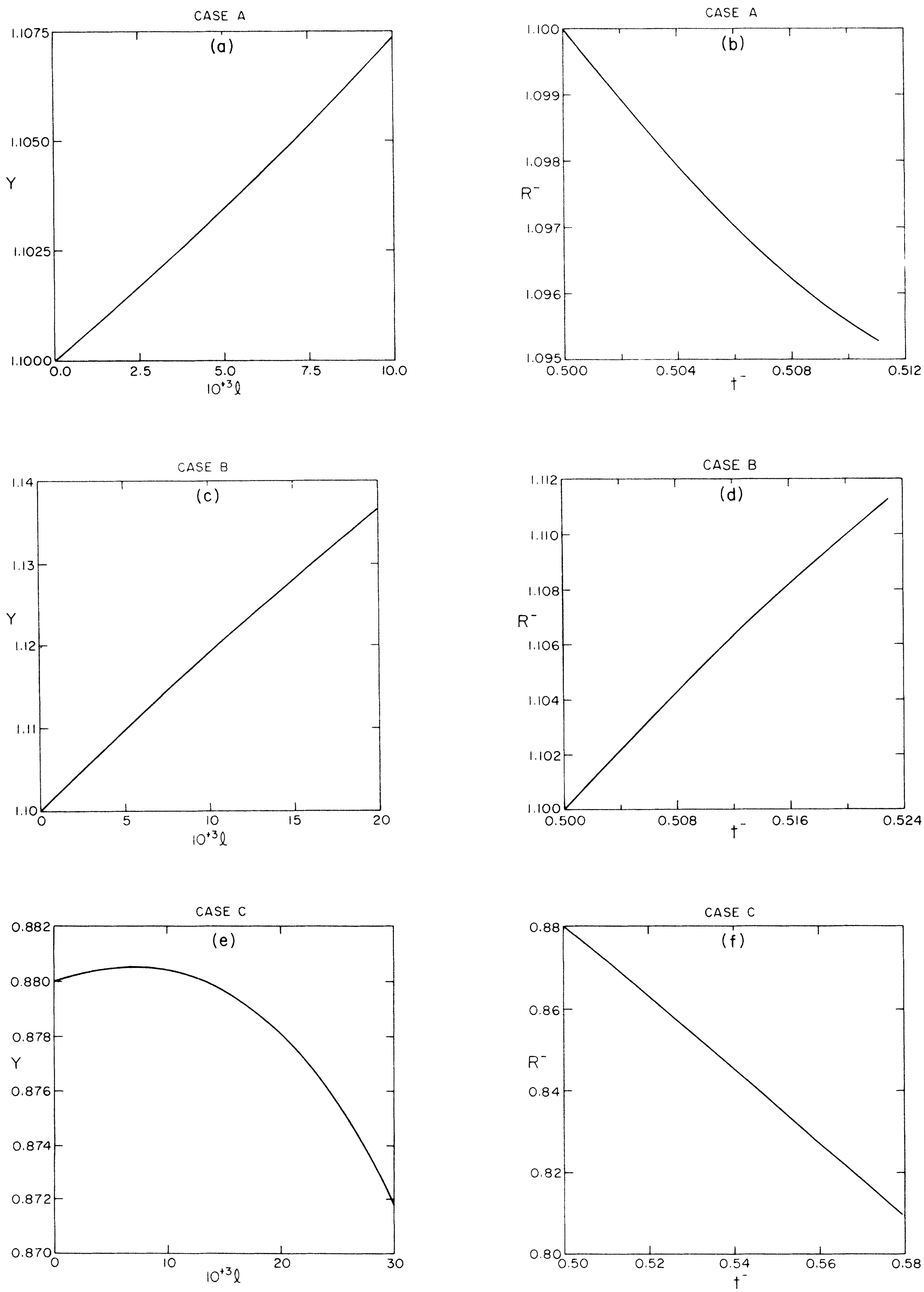

FIG. 5. Numerical solutions of Eqs. (4.17) and (4.18) for $Y(l)$ and $R^-(t^-)$, with $\tau=\pm\tilde{\epsilon}/2$ and $H(0)=1$ as the unit of length. The solutions correspond to each of the cases in Table I.

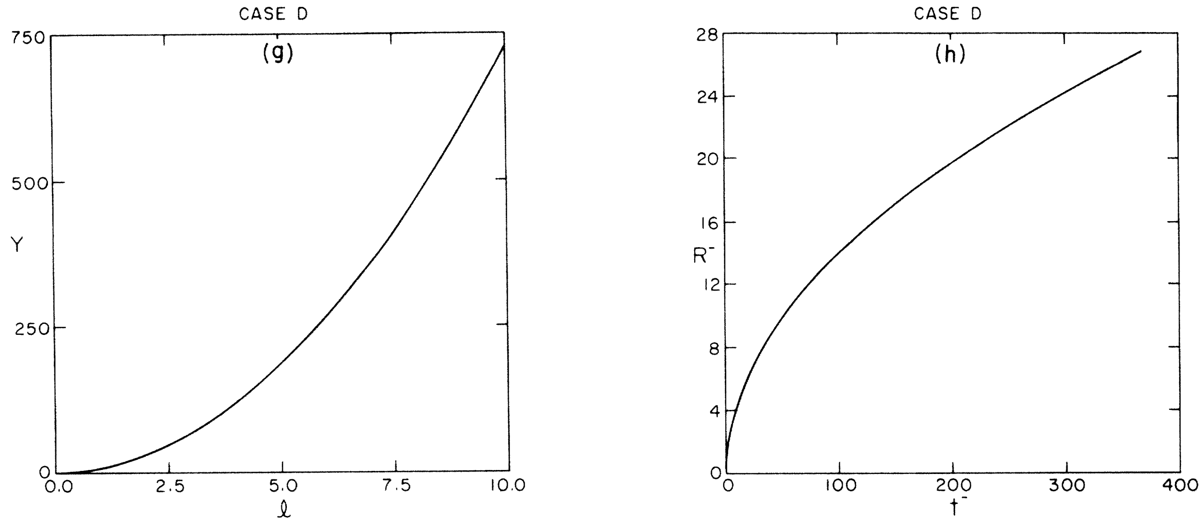

FIG. 5. (*Continued*).

V. CONCLUSIONS

For some particular cases we have analyzed the evolution and junction conditions of bubbles in general relativity with the inclusion of gravitational effects. Our initial motivation was to study the matching of the interior with the exterior space-time of a bubble in the old inflationary scenario since for such bubbles the thin wall approximation is valid, which allows the use of Israel's formalism for thin shells.

We made a review of Israel's formalism in Sec. II by obtaining the equations that solve Einstein's field equations for singular hypersurfaces of arbitrary shape. In Sec. III we introduced spherical symmetry and proceeded to find the equation of motion for a bubble immersed in a de Sitter space-time, which would be the case of a bubble in the original inflationary scenario. Results previously obtained by Lake[3] and Berezin, Kuzmin, and Tkachev[4] were derived and used to get the mapping $\mathscr{M}:\Sigma^+\mapsto\Sigma^-$ that effects the matching. Lemaitre-Robertson coordinates were required to have a complete description even beyond the event horizon of the de Sitter space-time.

In Sec. IV we deviated from our original motivation and analyzed a bubble immersed in a nonvacuum space-time although we still considered vacuum energy contributions. It was found that the assumptions of spatially flat FRW space-time in $M^{\pm}$ and vanishing energy density in the bubble's wall force a "worm-hole" matching of M^+ with M^-. In the particular case when this bubble expands following a Hubble law and the medium in M^- is massless radiation $p^-=\mu^-/3$, the bubble grows up to a maximum radius. For that limit, the magnitude of the tension in the wall becomes infinite, M^+ experiences inflation, and the coordinate radius of the bubble and its velocity vanish in M^+.

Finally, we dropped the condition of a Hubble law expansion of the bubble and assumed instead that the tension in the shell is constant. We found that there exist three different types of solutions for this case, which depend on the topology of the matching and whether the tension is positive or negative. Numerical solutions were obtained which show that the bubble either expands, contracts, or grows up to a maximum radius and then shrinks.

Of course, the price that we paid to obtain analytical solutions for the bubbles herein considered is that these bubbles are not adequate for inflation cosmologies since, on the one hand, the thin wall approximation is not valid for the new inflation scenario and, on the other hand, the special topology of the matching would now allow these bubbles to solve the problems for which the old inflationary universe scenario was introduced. Nonetheless, we have found several new interesting topologies for solutions to the Einstein equations, and these analytical models are extremely valuable because they are so amenable to analytical treatment; particularly interesting is the possibility for the existence of worm-hole bubbles that match spatially flat FRW regions with different equations of state.

ACKNOWLEDGMENTS

We are grateful to Dr. G. F. R. Ellis for valuable discussions. P.L.C. was supported by a Consejo Nacional de Ciéncia y Tecnológia Grant No. 49104. This work was supported in part by a National Science Foundation Grant No. PHY 8404931.

[1]A. H. Guth, Phys. Rev. D **23**, 347 (1981).
[2]S. Coleman and F. De Luccia, Phys. Rev. D **21**, 3305 (1980).
[3]K. Lake, Phys. Rev. D **29**, 1861 (1984).
[4]V. A. Berezin, V. A. Kuzmin, and I. I. Tkachev, Phys. Lett. **120B**, 91 (1983).
[5]S. W. Hawking, I. G. Moss, and J. M. Stewart, Phys. Rev. D **26**, 2661 (1982).
[6]W. Z. Chao, Phys. Rev. D **28**, 1898 (1983).

[7]V. A. Berezin, V. A. Kuzmin, and I. I. Tkachev, Phys. Lett. **130B**, 23 (1983).

[8]W. Israel, Nuovo Cimento **44B**, 1 (1966); **49B**, 463(E) (1967).

[9]A. D. Linde, Phys. Lett. **180B**, 389 (1982).

[10]C. W. Misner, K. S. Thorne, and J. A. Wheeler, *Gravitation* (Freeman, San Franciso, 1973).

[11]D. Kramer, H. Stephani, M. MacCallum, and E. Herlt, in *Exact Solutions of Einstein's Field Equations,* edited by E. Schmutzer (Deutscher Verlag, Berlin, 1980).

[12]V. A. Berezin, V. A. Kuzmin, and I. I. Tkachev, Phys. Lett. **124B**, 479 (1983).

[13]V. A. Berezin, V. A. Kuzmin, and I. I. Tkachev, Zh. Eksp. Teor. Fiz. **86**, 785 (1985) [Sov. Phys. JETP **59**, 459 (1984)].

[14]S. Coleman, Phys. Rev. D **15**, 2929 (1977).

[15]Ya B. Zel'dovich, I. Yo Kobzarev, and L. B. Okun, Zh. Eksp. Teor. Fiz. **67**, 3 (1974) [Sov. Phys. JETP **40**, 1 (1975)].

[16]S. W. Hawking and G. F. R. Ellis, *The Large Scale Structure of Space-Time* (Cambridge University Press, Cambridge, England, 1973).

[17]A. Aurilia, G. Denardo, F. Legovini, and E. Spallucci, Nucl. Phys. **B252**, 523 (1985).

[18]K. Lake and R. Wevrick, Can. J. Phys. **64**, 165 (1986).

[19]P. J. Steinhardt, Phys. Rev. D **25**, 2074 (1982).

[20]K. Maeda, K. Sato, M. Sasaki, and H. Kodama, Phys. Lett. **108B**, 98 (1982).

[21]K. Lake and R. Pim, Astrophys. J. **298**, 439 (1985); **304**, 75 (1986).

[22]H. Sato, in *General Relativity and Gravitation,* edited by B. Bertotti, F. de Felica, and A. Pascalini (Reidel, Boston, 1984).